0026-895X/96/020334-08$3.00/0

MOLECULAR PHARMACOLOGY, 50:334–341 (1996).

Attenuation of Inducible Nitric Oxide Synthase Gene Expression by Δ^9-Tetrahydrocannabinol Is Mediated through the Inhibition of Nuclear Factor-κB/Rel Activation

YOUNG J. JEON, KYU-H. YANG, JIM T. PULASKI, and NORBERT E. KAMINSKI

Departments of Pharmacology and Toxicology and Pathology, Michigan State University, East Lansing, Michigan (J.T.P., N.E.K.), and Department of Biological Sciences, Korea Advanced Institute of Science and Technology, Taejon, Korea (Y.J.J., K.-H.Y.)

Received March 5, 1996; Accepted May 2, 1996

SUMMARY

Δ^9-Tetrahydrocannabinol (Δ^9-THC), a prototypic compound belonging to the family of agents known as cannabinoids, produces a wide variety of biological effects, including inhibition of immune function. The putative mechanism for cannabinoid biological action involves binding to cannabinoid receptor types 1 and 2 (CB1 and CB2) to negatively regulate adenylate cyclase and inhibit intracellular signaling via the cAMP cascade. In the current study, we show that Δ^9-THC produces a marked inhibition of inducible nitric oxide synthase (iNOS) transcription and nitric oxide production by the macrophage line RAW 264.7 in response to lipopolysaccharide (LPS). Analysis of RAW 264.7 cell RNA demonstrated transcripts for CB2 but not CB1. Treatment of RAW 264.7 with Δ^9-THC inhibited forskolin-stimulated cAMP production in a dose-related manner, verifying the expression of functional cannabinoid receptors by this cell line. iNOS transcription, which is regulated in part by the nuclear factor-κB/Rel (NF-κB/Rel) family of transcription factors, has been shown to be under the control of the cAMP signaling cascade. We demonstrate that Δ^9-THC inhibits the activation and binding of NF-κB/Rel proteins to their cognate DNA site, κB, in response to LPS stimulation. LPS treatment of RAW 264.7 cells also induced the activation of the cAMP cascade, as indicated by an increase in binding of nuclear factors to the cAMP response element. Activation of CRE binding proteins was inhibited by Δ^9-THC. Forskolin treatment of RAW 264.7 cells induced both κB and cAMP response element binding activity and was likewise inhibited by Δ^9-THC. Collectively, this series of experiments indicates that NF-κB/Rel is positively regulated by the cAMP cascade to help initiate iNOS gene expression in response to LPS stimulation of macrophages. This activation of iNOS is attenuated by Δ^9-THC through the inhibition of cAMP signaling.

Currently, two major types of cannabinoid receptors, CB1 and CB2, have been isolated and cloned. Both receptors are involved in mediating the diverse biological actions of cannabinoid compounds, including immune suppression and alterations in central nervous system function. CB1 is expressed in greatest abundance within the brain (1, 2) but is also present at low levels in peripheral tissues, notably in spleen (3). CB2 has been identified only within the immune system (4). Both receptor types are negatively coupled to adenylate cyclase through a pertussis toxin-sensitive G protein (5) and inhibit the cAMP signaling cascade. Structure-activity studies show a strong correlation among the magnitude of inhibition by cannabinoids on adenylate cyclase activity, their binding affinity, and their respective rank order of potency in modifying biological responses (6).

Although the mechanism for immune suppression by cannabinoids has not been clearly established, disruption of the cAMP signaling cascade initiated by receptor/ligand interaction is a critical event in the suppression of a number of immune responses. This is made evident by the ability of membrane-permeable cAMP analogs to reverse cannabinoid-mediated inhibition of immune responses, including the anti-sheep erythrocytes IgM antibody-forming cell response and lymphoproliferation (6). Similarly, ADP-ribosylation of inhibitory G proteins in splenocytes by pertussis toxin blocks cannabinoid inhibition of both adenylate cyclase activity and antibody-forming cell responses (6). Cannabinoid receptor expression has been identified in all of the major immunological cells types, including B and T cells, monocytes, and

This work was supported by funds from National Institute on Drug Abuse Grants DA07908 and DA09171.

ABBREVIATIONS: CB1, cannabinoid receptor type 1; CB2, cannabinoid receptor type 2; Δ^9-THC, Δ-9-tetrahydrocannabinol; PMA, phorbol-12-myristate-13-acetate; RPMI 1640, Roswell Park Memorial Institute 1640; bp, base pair(s); RT-PCR, reverse transcription-polymerase chain reaction; iNOS, inducible nitric oxide synthase; CRE, cAMP response element; NF-κB, nuclear factor for immunoglobulin κ chain in B cells; LPS, lipopolysaccharide; NO, nitric oxide; PKA, cAMP-dependent protein kinase; PDTC, pyrrolidine dithiocarbamate; IS, internal standard; EMSA, electrophoretic mobility shift assay; BSA, bovine serum albumin; CREB; cAMP response element binding protein; ATF, activating transcription factor; IFN-γ, interferon-γ; HEPES, 4-(2-hydroxyethyl)-1-piperazineethanesulfonic acid.

mast cells, providing a rationale for the sensitivity of the immune system to modulation by cannabinoids (3, 4, 7, 8). Furthermore, it is likely that immunocellular responses regulated by cAMP signaling will exhibit sensitivity to cannabinoids and account for the wide range of immunological responses effected by this class of compounds.

We investigated the effect of Δ^9-THC on the LPS-induced NO response in macrophages, an important aspect of inflammation and innate host defense to bacterial pathogens. Stimulation of murine macrophages by LPS results in the expression of an iNOS, which catalyzes the production of large amounts of NO from L-arginine and molecular oxygen (9). NO, in turn, participates in the cytolytic function of macrophages (10). The promoter of the murine gene encoding iNOS contains two κB binding sites, located at 55 and 971 bp upstream of the TATA box, respectively (11). It has been reported that protein binding to the κB site is necessary to confer inducibility by LPS (12). The NF-κB/Rel family of transcription factors are pleiotropic regulators of many genes involved in immune and inflammatory responses, including iNOS (12, 13). NF-κB/Rel exists in the cytoplasm of unstimulated cells in a quiescent form bound to its inhibitor, IκB. Macrophage activation by certain external stimuli results in the phosphorylation of IκB by PKA, thus releasing the active DNA-binding form of NF-κB/Rel to translocate to the nucleus to bind κB motifs in the regulatory region of a variety of genes (14). LPS treatment of macrophages activates both protein kinase C and PKA, the latter being induced by an elevation of intracellular cAMP (15, 16). Also, interleukin-1, an inflammatory cytokine induced by LPS, contributes to the elevation of cAMP. The coordinate activation mediated through LPS and interleukin-1 is followed by increased iNOS expression and nitrite formation (17, 18). These results suggest that (a) the cAMP signaling cascade is involved in both NF-κB/Rel activation and iNOS induction after LPS stimulation and (b) the LPS-induced NO response is a likely candidate for modulation by cannabinoids. Here, we examine the role of cAMP signaling on LPS-induced iNOS activity and NO formation in the macrophage cell line RAW 264.7 by using the adenylate cyclase inhibitor Δ^9-THC.

Materials and Methods

Reagents. Δ^9-THC was provided by the National Institute on Drug Abuse (National Institutes of Health, Rockville, MD). LPS, PDTC, and 8-bromo-cAMP were purchased from Sigma Chemical (St. Louis, MO); forskolin was purchased from CalBiochem (La Jolla, CA); PCR reagents were purchased from Promega (Madison, WI); and reagents used for cell culture were purchased from GIBCO-BRL (Grand Island, NY).

Animals. Virus-free 4–6-week-old female B6C3F1 mice were purchased from the Frederick Cancer Research Center. On arrival, randomized mice were transferred to cages containing sawdust bedding (five mice/cage), given food (Purina Certified Lab Chow) and water *ad libitum*, and used for experimentation when their body weight was 17–20 g. Animal holding rooms were maintained at 21–24° and 40–60% relative humidity with a 12-hr light/dark cycle.

Cell culture. The peritoneal macrophages and RAW 264.7 cells (No. TIB-71; American Type Culture Collection, Rockville, MD) were grown in RPMI 1640 supplemented with 10% fetal bovine serum, 2 mM L-glutamine, 100 units/ml penicillin, and 100 μg/ml streptomycin. Peritoneal cells were harvested by sterile peritoneal lavage using Hanks' balanced salt solution, washed, resuspended in culture medium, and plated at 5×10^5 cells/ml. Nonadherent cells were removed by repeated washing after a 2-hr incubation at 37°.

Nitrite quantification. NO_2^- accumulation was used as an indicator of NO production in the medium as described previously (19). Peritoneal macrophages and RAW 264.7 cells were plated at 5×10^5 cells/ml onto 24-well culture plates and stimulated with LPS (200 ng/ml) in the presence or absence of Δ^9-THC (2.5. 5, 10, and 20 μM) for 24 hr. The isolated supernatants were mixed with an equal volume of Griess reagent (1% sulfanilamide, 0.1% naphthylethylene diamine dihydrochloride, 2% phosphoric acid) and incubated at room temperature for 10 min. Using $NaNO_2$ to generate a standard curve, nitrite production was measured by an absorbance reading at 550 nm.

Preparation of IS for RT-PCR. An artificial/recombinant mRNA (rcRNA) was used as an IS containing specific PCR primer sequences for iNOS that were added to RNA samples in a dilution series. A rat β-globin sequence was used as the spacer gene for the CB1, CB2, and iNOS IS. This method, developed by Vanden Heuvel, avoids sample-to-sample variation in reference gene expression (e.g., β-actin) as well as gene-to-gene differences in amplification efficiency (20, 21). The primer sequences from 5′ to 3′ for CB1 and CB2 are forward primer, ACCTGATGTTCTGGATCGGA; reverse primer, TGTTATCTAGAGGCTGCGCA; and forward primer, TTCTTACCTGCCGCTCATG; reverse primer, CGGATCTCTCCACTCCGTAG, respectively. The primer sequences from 5′ to 3′ for iNOS are forward primer, GGATAGGCAGAGATTGGAGG; and reverse primer, AATGAGGATGCAAGGCTGG. The CB1 and CB2 IS primer design from 5′ to 3′ is as follows: IS forward primer, T7 promoter (TAATACGACTCACTATAGG); CB1 or CB2 forward primer, as stated above; and rat β-globin forward primer, CCTGCAGTGTCTGATATTGTTG; and IS reverse primer, poly $d(T)_{18}$; CB1 or CB2 reverse primer, as stated above; and rat β-globin reverse primer, ACACACCATTGCGATGAA. The iNOS IS primer design from 5′ to 3′ is as follows: IS forward primer, T7 promoter; iNOS forward primer, as stated above; and rat β-globin forward primer, AAGCCTGGATACCAACCTGCC; and IS reverse primer, poly $d(T)_{18}$; iNOS reverse primer, as stated above; and rat β-globin reverse primer, AACCTGGATACCAACCTGCC. PCR reaction conditions for generating the IS were performed as stated previously using 100 ng of rat genomic DNA (21). PCR-amplified products were purified using the PCR Prep DNA purification system (Promega) and transcribed into RNA using the Gemini II *in vitro* transcription system (Promega). The rcRNA was subsequently treated with RNase-free DNase to remove the DNA template. After quantification, the IS concentration was calculated; 330 × bp is an approximation for the molecular weight of the IS, and the concentration is expressed in molecules of IS/μl.

Quantitative RT-PCR. RNA was isolated using Tri Reagent (Molecular Research Center, Cincinnati, OH) as described by Chomczynski and Mackey (22). To avoid any DNA contamination, RNA samples were incubated with RNase-free DNase for 15 min at 37° in 10 mM $MgCl_2$, 1 mM dithiothreitol, 25 units of RNasin, 10 mM Tris, and 1 mM EDTA. RNA was then extracted by phenol/chloroform and precipitated. Competitive RT-PCR was performed according to Gilliland *et al.* (23, 24), except that rcRNA was used as an IS instead of genomic DNA. Briefly, total RNA (100 ng) and IS rcRNA of known amount were reverse-transcribed into cDNA using oligo$(dT)_{15}$ as a primer. Eight aliquots of RNA were taken from each treatment groups, and an aliquot of IS rcRNA ranging from 10^3 to 10^{11} molecules was added to the appropriate treatment group RNA aliquot. A PCR mix consisting of PCR buffer (20 mM ammonium sulfate, 67 mM Tris, 6.7 μM EDTA, 80 μg/ml BSA, and 5 mM β-mercaptoethanol), 4 mM $MgCl_2$, 6 pmol each of iNOS forward and reverse primers, and 2.5 units of *Taq* DNA polymerase was added to the cDNA samples. Samples were then heated to 94° for 4 min and cycled 30 times at a 94° denaturing step for 15 sec, a 55° annealing step for 30 sec, and a 72° elongation step for 30 sec, after which an additional extension step at 72° for 5 min was included. PCR products were electrophoresed in 3% NuSieve 3:1 gels (FMC Bioproducts, Rockland, ME) and

visualized by ethidium bromide staining. The CB1, CB2, and iNOS primers produce amplified products at 450, 429, and 379 bp from the RNA sample and at 371, 370, and 301 bp from the IS rcRNA, respectively. Quantification was performed using the Gel Doc 1000 (Bio-Rad, Hercules, CA), with which the amount of target mRNA present is determined according to Gilliland *et al.* (23). For example, the ratio of the volume of the IS rcRNA to iNOS RNA band is plotted against the amount of IS rcRNA (in molecules) added to each reaction. The point at which the ratio of IS (rcRNA) to iNOS mRNA is equal to 1 is denoted the "cross-over" point and represents the amount of iNOS mRNA present in the initial RNA sample. After performance of the 10^3-10^{11} range-finding experiment, a second set of much-narrower IS dilutions (i.e., for iNOS 10^6-10^{10} molecules/tube) were examined to more accurately quantify RNA message levels.

EMSA. Nuclear extracts were prepared as described previously (25). Treated and untreated RAW 264.7 cells were lysed with hypotonic buffer (10 mM HEPES, 1.5 mM $MgCl_2$, pH 7.5), and the nuclei were pelleted by centrifugation at 3000 × *g* for 5 min. Nuclear lysis was performed using a hypertonic buffer (30 mM HEPES, 1.5 mM $MgCl_2$, 450 mM KCl, 0.3 mM EDTA, 10% glycerol) that contained 1 mM dithiothreitol, 1 mM phenylmethylsulfonyl fluoride, and 1 μg/ml concentration each of aprotinin and leupeptin. After lysis, the samples were centrifuged at 14,500 × *g* for 15 min, and the supernatant was retained for use in the DNA binding assay. Two double-stranded deoxyoligonucleotides containing the CRE (5′-TGACGTCA-3′) (26) and the NF-κB binding site (5′-GGGGACTTTCC-3′) (27) were end-labeled with [γ-^{32}P]dATP. Nuclear extracts (3 μg) were incubated with poly(dI-dC) (0.5 μg for CREB/ATF binding and 2 μg for NF-κB/Rel binding) and the ^{32}P-labeled DNA probe in binding buffer (100 mM NaCl, 30 mM HEPES, 1.5 mM $MgCl_2$, 0.3 mM EDTA, 10% glycerol, 1 mM dithiothreitol, 1 mM phenylmethylsulfonyl fluoride, 1 μg/ml concentration each of aprotinin and leupeptin) for 10 min on ice. DNA binding activity was separated from free probe using a 4.8% polyacrylamide gel in 1× Tris/Borate/EDTA buffer (89 mM Tris, 89 mM boric acid, 2 mM EDTA). After electrophoresis, the gel was dried and subjected to autoradiography.

cAMP determinations. RAW 264.7 cells were washed with RPMI 1640, resuspended in RPMI 1640 with 1 mg/ml fatty acid-poor BSA (CalBiochem), and adjusted to 5 × 10^5 cells/ml. One-milliliter aliquots of cells were treated with either vehicle (1% ethanol) or Δ^9-THC (2.5, 5, 10, and 20 μM) and then incubated for 10 min at room temperature. The appropriate cell preparations were then stimulated with 50 μM forskolin for 15 min at 37° in 5% CO_2. After stimulation, the adenylate cyclase was inactivated by the addition of the cAMP extraction buffer (95% ethanol, 0.01 N HCl). Supernatants were collected and dried. Aliquots of reconstituted cell lysates were quantified for cAMP using a cAMP assay kit (Diagnostic Products, Los Angeles, CA) (28).

Statistical analysis. Mean ± standard deviation values was determined for each treatment group in a given experiment. When significant differences occurred, treatment groups were compared with the vehicle controls using a Dunnett's two-tailed *t* test (29).

Results

Cannabinoid receptor expression. Expression of mRNA for the cannabinoid receptors CB1 and CB2 was quantified using RT-PCR. Total RNA of RAW 264.7 cells was prepared, reverse-transcribed into cDNA, and amplified by PCR using primers specific for the cDNA of interest. In RAW 264.7 cells, CB2 was highly expressed at ~1 × 10^5 molecules/100 ng RNA, whereas CB1 expression was undetectable.

Effect of Δ^9-THC on forskolin-stimulated adenylate cyclase activity in RAW 264.7 cells. The effect of Δ^9-THC on forskolin-stimulated adenylate cyclase activity was measured to indirectly verify whether RAW 264.7 cells express functional cannabinoid receptors (Fig. 1). Forskolin treatment alone markedly activated adenylate cyclase as demonstrated by a 10-fold elevation in intracellular cAMP compared with forskolin-unstimulated cells. Pretreatment of RAW 264.7 cells with Δ^9-THC before forskolin stimulation significantly decreased cAMP formation by 31%, 45%, and 84% at 5, 10, and 20 μM respectively. No effect on cell viability was observed in any of the treatment groups and always exceeded 85% as determined by eosin Y staining (data not shown).

Effects of Δ^9-THC on nitrite production and iNOS gene expression in macrophages. LPS (200 ng/ml) alone increased the production of nitrite ≥12-fold over basal levels in peritoneal macrophages and RAW 264.7 cells (Fig. 2). Basal levels of nitrite in unstimulated peritoneal macrophages and RAW 264.7 cells were <1 nmol/ml (mean ± standard deviation, three experiments). On LPS-stimulation, nitrite synthesis by peritoneal macrophages and RAW 264.7 cells increased by 13- and 26-fold, respectively. Furthermore, this induction in nitrite generation by LPS was inhibited by Δ^9-THC. Consistent with these finding, iNOS mRNA was not detectable in unstimulated RAW 264.7 cells. Conversely, RNA isolated from RAW 264.7 cells treated for 6 hr with LPS showed the active transcription of the iNOS gene as demonstrated by RT-PCR. Furthermore, Δ^9-THC (10 and 20 μM) inhibited LPS-induced iNOS transcription (Table 1). In this same series of experiments, it is notable that a very modest increase in iNOS transcript was observed in experiment 1 in the 5 μM Δ^9-THC-plus-LPS treatment group; however, we believe this was most likely due to biological variability because it was not observed in a subsequent experiment.

Because LPS treatment of macrophages activates both PKA and protein kinase C signaling pathways, RAW 264.7 cells were cotreated with PMA or 8-bromo-cAMP in the presence of LPS and Δ^9-THC (20 μM) for 24 hr to identify which

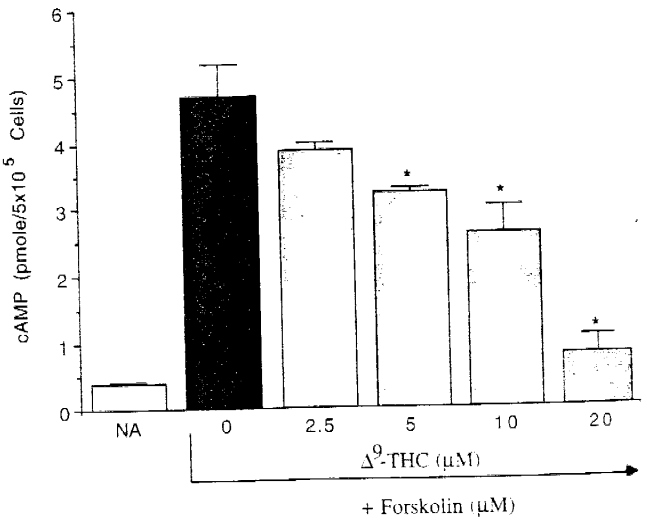

Fig. 1. Inhibition of cAMP production by Δ9-THC in forskolin-stimulated RAW 264.7 cells. RAW 264.7 cells at 5 × 10^5 cells/ml were incubated with either vehicle (0.1% ethanol) or Δ^9-THC (2:5, 5, 10, and 20 μM) for 10 min, followed by a 15-min stimulation with forskolin (50 μM). Intracellular cAMP concentrations are expressed as the mean ± standard deviation of triplicate determinations. *, Response that is significantly different from the control group as determined by Dunnett's two-tailed *t* test at $p < 0.05$. One of two representative experiments is shown.

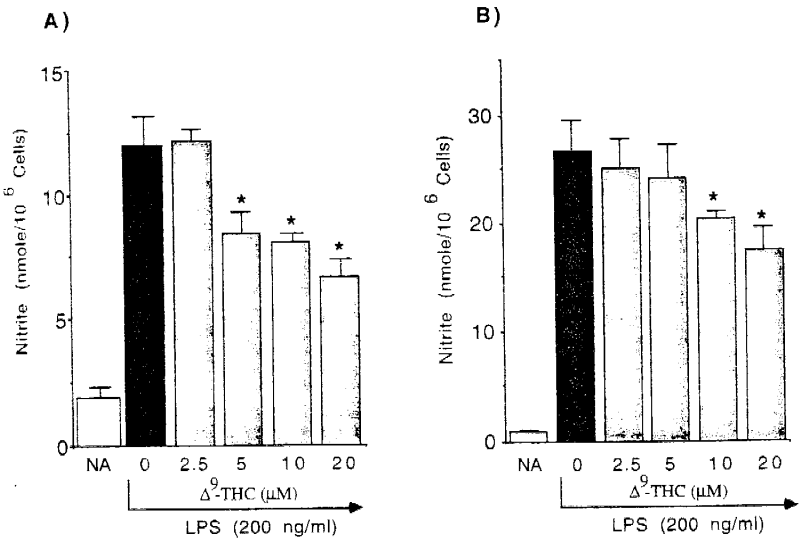

Fig. 2. Inhibition of nitrite production by Δ^9-THC in LPS-stimulated peritoneal cells and RAW 264.7 cells. Peritoneal adherent cells (A) and RAW 264.7 cells (B) were treated with Δ^9-THC (2.5, 5, 10, and 20 μM) in the presence of LPS (200 ng/ml) for 24 hr. The supernatants were subsequently isolated and analyzed for nitrite. *Bars*, mean ± standard deviation of triplicate determinations. *, Response that is significantly different from the control group as determined by Dunnett's two-tailed *t* test at $p < 0.05$. One of two representative experiments is shown.

TABLE 1

Inhibition of iNOS gene expression by Δ^9-THC in LPS-stimulated RAW 264.7 cells

RAW 264.7 cells were treated with Δ^9-THC (2.5, 5, 10, and 20 μM) in the presence of LPS (200 ng/ml) for 6 hr. Total RNA was isolated and the molecules of iNOS mRNA were quantitated as outlined in Materials and Methods.

Treatment	iNOS	
	Experiment 1	Experiment 2
	molecules × 10^7/100 ng RNA	
NA	N.D.	N.D.
LPS	5.89	10.4
LPS + Δ^9-THC (2.5 μM)	6.05	6.41
LPS + Δ^9-THC (5 μM)	6.62	4.73
LPS + Δ^9-THC (10 μM)	3.82	4.29
LPS + Δ^9-THC (20 μM)	3.65	2.27

N.D., not detectable.

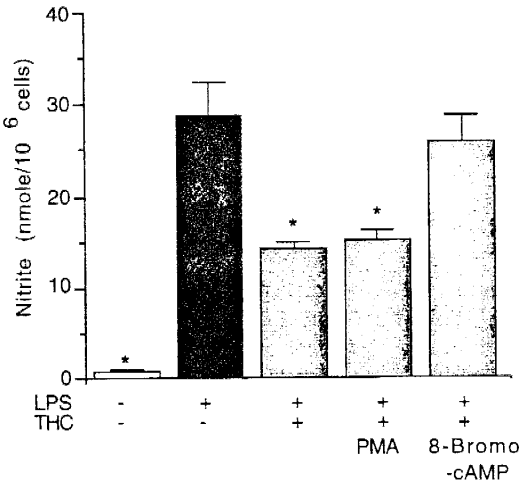

Fig. 3. Reversal of Δ^9-THC-mediated inhibition of nitrite production in LPS-stimulated RAW 264.7 cells by 8-bromo-cAMP. RAW 264.7 cells were treated with PMA or 8-bromo-cAMP in the presence of LPS (200 ng/ml) and Δ^9-THC (20 μM) for 24 hr. The supernatants were subsequently isolated and analyzed for nitrite. *Bars*, mean ± standard deviation, triplicate determinations; *, Significant difference from the control group as determined by Dunnett's two-tailed *t* test at $p < 0.05$. One of two representative experiments is shown.

of the two potential signaling pathways may be involved in the inhibition of nitric oxide production by cannabinoids (Fig. 3). 8-bromo-cAMP, a membrane-permeable cAMP analog, but not PMA restored nitrite production in the presence of Δ^9-THC.

Inhibition of NF-κB/Rel binding activity by Δ^9-THC treatment in LPS-stimulated RAW 264.7 cells. It has been reported that protein binding at the κB binding site is necessary to confer inducibility by LPS of iNOS (12). In the present series of experiments, we investigated the role of adenylate cyclase inhibition by Δ^9-THC on regulation of NF-κB/Rel and the relationship between NF-κB/Rel and LPS-induced iNOS gene expression. Our initial studies demonstrated that LPS (200 ng/ml) treatment of RAW 264.7 cells induced a marked increase in NF-κB/Rel binding to its cognate site at 1 and 2 hr, which could be visualized as two distinct bands (Fig. 4). This banding pattern was similar to that previously described by Xie *et al.* (12). In their study, the upper band was composed of p50/RelA(p65) and p50/c-rel heterodimers, whereas the lower band consisted of a p50 homodimer as identified by gel supershift assays (12). In the presence of Δ^9-THC, LPS-induced NF-κB/Rel binding was noticeably inhibited at 1 and 2 hr, and this inhibition by Δ^9-THC was dose related, as shown in Fig. 4B. To confirm the involvement of NF-κB/Rel in the induction of iNOS gene expression by LPS-stimulated RAW 264.7 cells, we used PDTC, an antioxidant that inhibits NF-κB/Rel activation (30). Concomitant treatment of RAW 264.7 cells with PDTC and LPS significantly inhibited NF-κB/Rel binding activity (Fig. 5A). Under identical conditions (i.e., preincubation with PDTC), LPS-activated RAW 264.7 cells exhibited a dose-dependent inhibition in nitrite generation, confirming the involvement of NF-κB/Rel in LPS-induced nitrite generation (Fig. 5B). Collectively, this series of experiments indicates that NF-κB/Rel is positively regulated by the cAMP cascade to help initiate iNOS gene expression in response to LPS.

Activation of CREB/ATF binding with LPS in RAW 264.7 cells. In addition to the regulation of NF-κB/Rel, the cAMP signaling cascade is best known for its activation of the CREB/ATF family of DNA binding proteins. Because Δ^9-THC inhibits cAMP signaling through the inhibition of adenylate cyclase, the present series of experiments were performed to investigate whether CREB/ATF DNA binding factors are activated by LPS stimulation of macrophages and, if so,

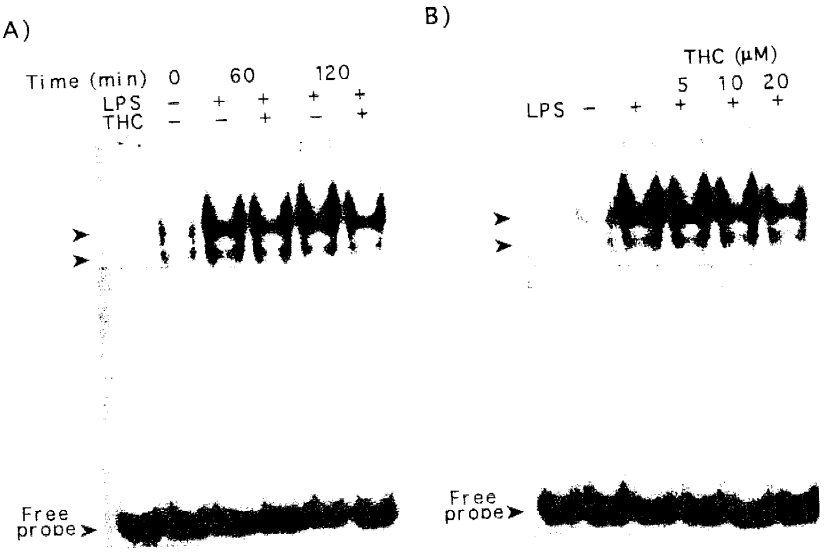

Fig. 4. Inhibition of NF-κB/Rel binding by Δ^9-THC in LPS-stimulated RAW 264.7 cells. RAW 264.7 cells were treated with (A) Δ^9-THC (20 μM) in the presence of LPS (200 ng/ml) for 1 or 2 hr or (B) Δ^9-THC (2.5, 5, 10, and 20 μM) for 2 hr. Nuclear extracts were then prepared and subjected to EMSA. *Arrowheads*, NF-κB/Rel binding. Results are representative of three separate experiments.

whether their regulation would also be adversely affected by Δ^9-THC. Nuclear extracts were prepared from RAW 264.7 cells stimulated with LPS (200 ng/ml) for various lengths of time (0–2.5 hr) and then subjected to EMSA using a CRE double-stranded oligonucleotide, the cognate binding site for the CREB/ATF family of nuclear factors. RAW 264.7 cells were found to express a moderate constitutive level of CRE binding activity before LPS stimulation that substantially increased 1 hr after LPS treatment and peaked at 1.5 hr. By 2.5 hr after LPS stimulation, CRE binding decreased to basal levels (Fig. 6A). CRE binding was visualized as two bands: a major bottom band and a minor top band that was only apparent in LPS-activated RAW 264.7 cells. In the presence of Δ^9-THC (20 μM), LPS-induced CRE binding was diminished at 1 and 2 hr with almost complete abrogation of the minor band (Fig. 6B). The specificity of the retarded bands was confirmed by the addition of an excess of ^{32}P-unlabeled double-stranded CRE oligonucleotide that competed for protein binding (Fig. 6C).

Effects of Δ^9-THC on NF-κB/Rel and CREB/ATF binding activity in forskolin-stimulated RAW 264.7 cells. To further characterize the role of the cAMP signaling cascade in the modulation of nuclear factor binding to κB and CRE motifs, RAW 264.7 cells were treated with forskolin, an agent that elevates cAMP by directly activating adenylate cyclase. As shown in Fig. 7, both NF-κB/Rel and CREB/ATF bindings were enhanced at 30 and 60 min after forskolin treatment. However, stimulation of cells with forskolin in the presence of Δ^9-THC (20 μM) resulted in the inhibition of nuclear factor binding to both κB and CRE.

Discussion

We demonstrated that Δ^9-THC treatment significantly attenuates LPS-induced iNOS transcription through an inhibition of the cAMP signaling cascade in the macrophage line RAW 264.7. As previously shown by a number of researchers, including ourselves, lymphoid and myeloid cells express cannabinoid receptors (3, 4, 7, 8, 31), which negatively regulate adenylate cyclase and lead to a decrease in cellular cAMP (6, 32, 33). Ligand binding to these receptors by cannabinoids represents one of the putative mechanisms by which this class of compounds exerts their broad range of biological effects, including immune suppression. Although the relative distribution of this family of receptors on specific cell types within the immune system has not been widely studied, radioligand binding analysis indicates that there are ~1000 receptor binding sites in mouse spleen cell preparations (3). Progress has been made in describing which of the two cannabinoid receptor types, CB1 and/or CB2, is expressed within the immune system and other tissues. Results of radioligand binding, Northern analysis, and structure-activity relationship studies strongly suggest that CB2 is the predominant form of cannabinoid receptor expressed within the immune system (3, 4, 7, 31). It is notable that CB1, although exhibiting low expression at the transcriptional level, has been identified in a variety of immunological preparations by RT-PCR (3, 7). In these experiments, examination of RAW 264.7 cell RNA by quantitative RT-PCR revealed transcripts for CB2 only and no detectable CB1. The functionality of cannabinoid receptors in RAW 264.7 cells was verified by the ability of Δ^9-THC to inhibit forskolin-stimulated cAMP accumulation in a dose-related manner.

Recently, it was demonstrated that initiation of iNOS transcription is under the control of the cAMP cascade. Treatment of various cell preparations, including rat peritoneal macrophages (18) and vascular smooth muscle cells (17), with membrane-permeable cAMP analogs (dibutyryl-cAMP and 8-bromo-cAMP) or with forskolin resulted in an augmentation in NO synthesis. Most pertinent to our studies, it has been shown in macrophages that induction of NO by insoluble complexes of monoclonal IgE anti-dinitrophenol antibody and dinitrophenol-BSA is mediated through an increase in iNOS expression that is independent of elevations in either cytosolic calcium or protein tyrosine phosphorylation (18). Consistent with these findings, our experiments show that Δ^9-THC, at concentrations that inhibit adenylate cyclase, simultaneously inhibits LPS-induced NO production in both RAW 264.7 cells and peritoneal macrophages. Furthermore, this cannabinoid-mediated inhibition of NO production can be abrogated by concomitant treatment of RAW 264.7 cells with 8-bromo-cAMP but not with phorbol ester. These findings suggest the involvement of the cAMP cascade in the

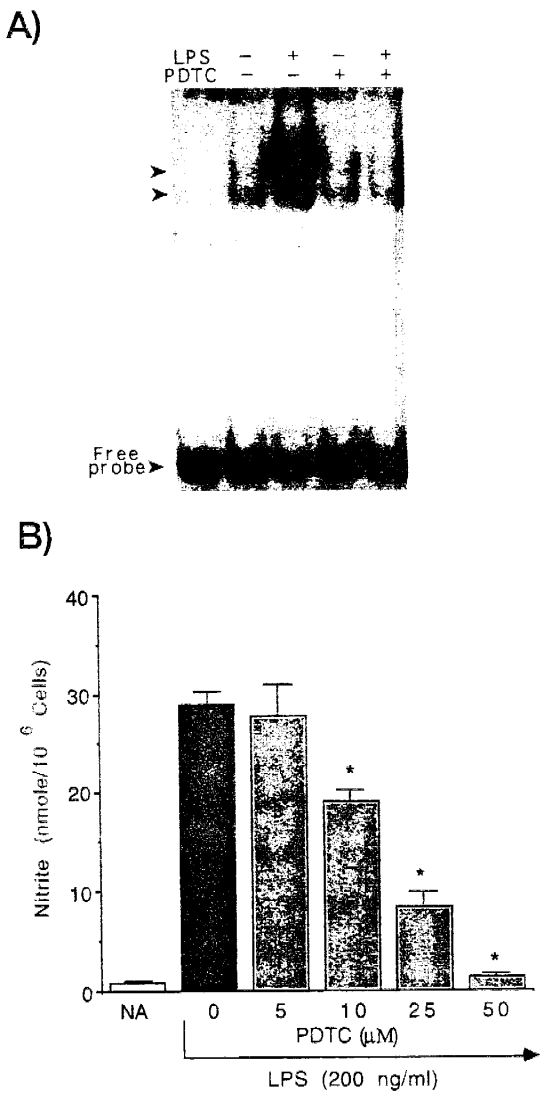

Fig. 5. Inhibition of NF-κB/Rel binding and nitrite production by PDTC in LPS-stimulated RAW 264.7 cells. A, RAW 264.7 cells were treated with PDTC (50 μM) in the presence or absence of LPS (200 ng/ml) for 2 hr. Nuclear extracts were then prepared and subjected to EMSA. *Arrowheads*, NF-κB/Rel binding. B, RAW 264.7 cells were treated with PDTC (5, 10, 25, and 50 μM) in the presence of LPS (200 ng/ml) for 24 hr. The supernatants were subsequently isolated and analyzed for nitrite. Each bar represents the mean ± standard deviation for triplicate determinations. *, Significant difference from the control group as determined by Dunnett's two-tailed *t* test at $p < 0.05$. Results are representative of three separate experiments.

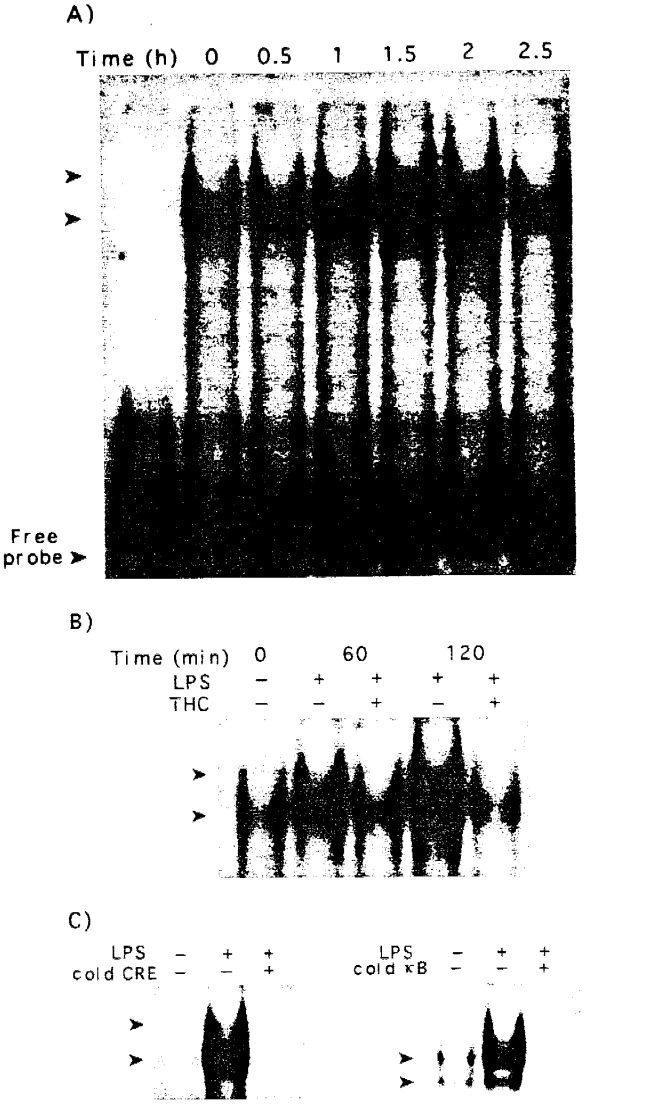

Fig. 6. Δ^9-THC-mediated inhibition of CREB/ATF binding in LPS-stimulated RAW 264.7 cells. A, Nuclear extracts from LPS (200 ng/ml)-stimulated RAW 264.7 cells were incubated with ^{32}P-labeled CRE probe. B, RAW 264.7 cells were treated with Δ^9-THC (20 μM) in the presence of LPS. C, In competition studies, 1 pmol of unlabeled κB or CRE was added to the reaction mixture. Reaction products were electrophoresed, and the gels were dried and autoradiographed. *Arrowheads*, CREB/ATF binding. Results are representative of three separate experiments.

regulation of iNOS by RAW 264.7 cells as previously suggested by studies in rat peritoneal macrophages (18).

The activation of NO production is closely tied to transcriptional activation of iNOS. Insight into the regulation of the iNOS gene comes from the results of recent studies that have identified several known nuclear regulatory factor recognition motifs within the iNOS promoter region. Deletion analysis of the iNOS promoter using luciferase reporter constructs identified two regions that significantly increased luciferase activity in RAW 264.7 cells after LPS treatment (termed regions I and II) (11). Region I (position −48 to −209) contains binding motifs for NF-κB and NF-interleukin-6 and was found to be essential for luciferase activity. Region II (position −913 to −1029) contains motifs for binding IFN-γ-related transcription factors (IFN-stimulated response element and Pu.1/IFN-γ element) as well as a κB motif. Constructs containing region II alone exhibited no activity in LPS-activated RAW 264.7 cells. Constructs containing both regions I and II exhibited a greater magnitude of activity than found in region I alone, and activity was further enhanced by cotreatment with IFN-γ. These studies suggest that region II functions as an enhancer for region I. The involvement of NF-κB/Rel family member proteins in iNOS gene regulation by macrophages in response to LPS-stimulation was confirmed by gel shift studies and iNOS luciferase constructs using RAW 264.7 cells (12). Deletion of κB motifs from iNOS constructs resulted in the abrogation of luciferase activity after LPS treatment (12). Gel shift and supershift studies demonstrated that LPS treatment induced a rapid

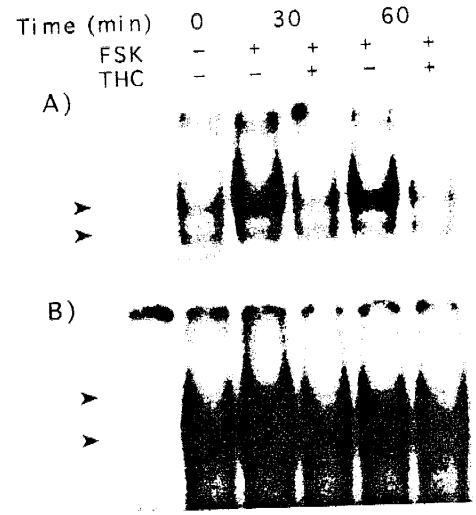

Fig. 7. Inhibition of NF-κB/Rel and CREB/ATF binding by Δ^9-THC in forskolin-stimulated RAW 264.7 cells. RAW 264.7 cells were treated with Δ^9-THC (20 μM) in the presence of forskolin (50 μM) for 30 or 60 min. Nuclear extracts were then prepared and incubated with ^{32}P-labeled (A) κB probe or (B) CRE probe. Reaction products were electrophoresed, and the gels were dried and autoradiographed. *Arrowheads*, CREB/ATF and NF-κB/Rel binding. Results are representative of three separate experiments.

(≤30 min) and persistent (measurable at 2 hr) activation of several NF-κB/Rel family member complexes, including heterodimers of p50/c-rel, p50/Rel A(p65), and p50/p50 homodimers (12). As discussed, our experiments show that Δ^9-THC effectively inhibits LPS activation of iNOS transcription and NO activity in RAW 264.7 cells. To further investigate the putative mechanism by which cannabinoids inhibit iNOS, we chose to monitor the effects of cannabinoid compounds on the activation of two families of transcription factors by gel shift assays during LPS activation of macrophages. NF-κB/Rel family member binding activity was examined in light of their critical role in the regulation of iNOS. Also, CREB/ATF binding was monitored as a measure of inhibition of the cAMP signaling cascade by cannabinoids. Kinetics studies showed strong induction by LPS of two separate κB binding complexes at 60 min and more enhanced induction at 120 min. Δ^9-THC inhibited the activation of both of these κB binding complexes; however, the magnitude of inhibition seemed to be greater for the protein complex represented by the top of the two bands. This finding suggests that Δ^9-THC may inhibit the formation of either p50/c-rel or p50/Rel A(p65) heterodimers based on the study by Xie *et al.* (12) in which the authors identified these NF-κB/Rel proteins as being responsible for this top band. Our experiments verified that the inhibition of LPS-induced κB binding by Δ^9-THC was dose dependent and that the binding was κB specific as demonstrated by competition assays with ^{32}P-unlabeled κB probe. Additional control experiments were performed to verify a role for NF-κB/Rel family members in iNOS regulation using the PDTC, an inhibitor of NF-κB activation, in our LPS-treated RAW 264.7 cell preparations (30). PDTC effectively inhibited the activation of NF-κB/Rel binding complexes and NO production.

Because of the inhibitory effects that cannabinoids exert on the cAMP formation and signaling coupled with the fact that LPS-induced NF-κB activation has been reported to be primarily regulated by PKA (14, 15, 34), our experiments also focused on cAMP signaling. Treatment of RAW 264.7 cells with either LPS or the adenylate cyclase activator forskolin resulted in the activation of CRE binding proteins. Both activation stimuli induced two CRE binding complexes that were visualized as a minor (top) and a major (bottom) band in gel shift assays. Likewise, activation of RAW 264.7 cells with either stimuli (i.e., LPS or forskolin) in the presence of Δ^9-THC resulted in a decrease in CRE binding of both of the DNA binding complexes and is indicative that Δ^9-THC produces an inhibition in the cAMP signaling cascade. Furthermore, concordant with previous studies suggesting that PKA is responsible for the activation of NF-κB/Rel as shown in macrophages (14, 15) and B cells (34), treatment of RAW 264.7 cells with forskolin resulted in the activation of NF-κB binding that was also attenuated by Δ^9-THC. Additional evidence that cAMP signaling is involved in LPS-induced responses by macrophages was provided by the activation of CRE binding after LPS treatment of RAW 264.7 cells. This LPS-induced activation of CRE DNA binding proteins peaked at ~90–120 min after LPS treatment and resulted in a similar banding pattern to that observed after forskolin-stimulation. Taken together, our findings strongly suggest that NF-κB/Rel is activated by the cAMP signaling cascade by PKA-mediated phosphorylation of the NF-κB inhibitory protein, IκB (35).

In summary, these experiments demonstrate that Δ^9-THC inhibits LPS-induced activation of iNOS in macrophages and NO production. Based on our findings, the most likely mechanism that can account for this biological effect involves the inhibition of cAMP formation through negative regulation of adenylate cyclase by G protein-coupled cannabinoid receptors. Inhibition of the cAMP signaling cascade attenuates the activation of NF-κB binding proteins, which are necessary for the activation of the iNOS gene. At least two significant points are brought out by these studies. First, these experiments further confirm the critical role of cAMP signaling in the regulation of iNOS via NF-κB. Furthermore, due to the critical role that NO release plays in mediating inflammatory responses, the inhibitory effects of cannabinoids on iNOS suggest that this family of compounds may represent a useful new class of anti-inflammatory agents. This is further supported by our recent findings that cannabinoid compounds also inhibit interleukin-2, a critical mediator of T cell clonal expansion (36).

References

1. Herkenham, M., A. B. Lynn, M. D. Little, M. R. Johnson, L. S. Melvin, B. R. de Costa, and K. C. Rice. Cannabinoid receptor localization in brain. *Proc. Natl. Acad. Sci. USA* **87:**1932–1936 (1990).
2. Thomas, B. F., X. Wei, and B. R. Martin. Characterization and autoradiographic localization of the cannabinoid binding site in rat brain using [^{3}H]11-OH-Δ^9-THC-DMH. *J. Pharmacol. Exp. Ther.* **263:**1383–1390 (1992).
3. Kaminski, N. E., M. E. Abood, F. K. Kessler, B. R. Martin, and A. R. Schatz. Identification of a functionally relevant cannabinoid receptor on mouse spleen cells that is involved in cannabinoid-mediated immune modulation. *Mol. Pharmacol.* **42:**736–742 (1992).
4. Munro, S., K. L. Thomas, and M. Abu-Shaar. Molecular characterization of a peripheral receptor for cannabinoids. *Nature (Lond.)* **365:**61–65 (1993).
5. Matsuda, L. A., S. J. Lolait, M. J. Brownstein, A. C. Young, and T. I. Bonner. Structure of a cannabinoid receptor and functional expression of the cloned cDNA. *Nature (Lond.)* **346:**561–564 (1990).
6. Kaminski, N. E., W. S. Koh, M. Lee, K. H. Yang, and F. K. Kessler. Suppression of the humoral immune response by cannabinoids is partially mediated through inhibition of adenylate cyclase by a pertussis toxin-sensitive G-protein coupled mechanism. *Biochem. Pharmacol.* **48:**1899–1908 (1994).

7. Bouaboula, M., M. Rinaldi, P. Carayon, C. Carillon, B. Delpech, D. Shire, G. Le Fur, and P. Casellas. Cannabinoid-receptor expression in human leukocytes. *Eur. J. Biochem.* **214:**173–180 (1993).
8. Facci, L., R. Dal Toso, S. Romanello, A. Buriani, D. Skaper, and A. Leon. Mast cells express a peripheral cannabinoid receptor with differential sensitivity to anandamide and palmitoylethanolamide. *Proc. Natl. Acad. Sci. USA* **92:**3376–3380 (1995).
9. Palmer, R. M. J., D. S. Ashton, and S. Moncada. Vascular endothelial cells synthesize nitric oxide from L-arginine. *Nature (Lond.)* **333:**664–666 (1988).
10. Hibbs, J. B., R. R. Taintor, and Z. Vavrin. Macrophage cytotoxicity: role for L-arginine deiminase and imino nitrogen oxidation to nitrite. *Science (Washington D. C.)* **235:**473–476 (1987).
11. Lowenstein, C. J., E. W. Alley, P. Raval, A. M. Snowman, S. H. Snyder, S. W. Russell, and W. J. Murphy. Macrophage nitric oxide synthase gene: two upstream regions mediate induction by interferon γ and lipopolysaccharide. *Proc. Natl. Acad. Sci. USA* **90:**9730–9734 (1993).
12. Xie, Q., Y. Kashiwabara, and C. Nathan. Role of transcription factor NF-κB/Rel in induction of nitric oxide synthase. *J. Biol. Chem.* **269:**4705–4708 (1994).
13. Grilli, M., J.-S. Chiu, and M. Lenardo. NF-κB and Rel: participants in a multiform transcriptional regulatory system, in *International Review of Cytology: A Survey of Cell Biology*. Academic Press, San Diego, 1–62 (1993).
14. Shirakawa, F., and S. B. Mizel. *In vitro* activation and nuclear translocation of NF-κB catalyzed by cyclic AMP-dependent protein kinase and protein kinase C. *Mol. Cell. Biol.* **9:**2424–2430 (1989).
15. Muroi, M., and T. Suzuki. Role of protein kinase A in LPS-induced activation of NK-κB proteins of a mouse macrophage-like cell-line, J774. *Cell. Signalling* **5:**289–298 (1993).
16. Novotney, M., Z.-L. Chang, H. Uchiyama, and T. Suzuki. Protein kinase C in tumoricidal activation of mouse macrophage cell lines. *Biochemistry* **30:**5597–5604 (1991).
17. Koide, M., Y. Kawahara, I. Nakayama, T. Tsuda, and M. Yokoyama. Cyclic AMP-elevating agents induce an inducible type of nitric oxide synthase in cultured vascular smooth muscle cells. *J. Biol. Chem.* **268:**24959–24966 (1993).
18. Alonso, A., J. Carvalho, S. Alonso-Torre, L. Nunez, L. Bosca, and M. Crespo. Nitric oxide synthesis in rat peritoneal macrophages is induced by IgE/DNP complexes and cyclic AMP analogues: evidence in favor of a common signaling mechanism. *J. Immunol.* **154:**6475–6483 (1995).
19. Green, L. C., D. A. Wagner, J. Glogowski, P. L. Skipper, J. S. Wishnok, and J. S. Tannenbaum. Analysis of nitrate, nitrite, and [^{15}N]nitrate in biological fluids. *Anal. Biochem.* **126:**131–138 (1982).
20. Vanden Heuvel, J., G. Clark, M. Kohn, A. Tritscher, W. Greenlee, G. Lucier, and D. Bell. Dioxin-responsive genes: examination of dose-response relationships using quantitative reverse transcriptase-polymerase chain reaction. *Cancer Res.* **54:**62–68 (1994).
21. Vanden Heuvel, J., F. Tyson, and D. Bell. Construction of recombinant RNA templates for use as internal standards in quantitative RT-PCR. *Biotechniques* **14:**395–398 (1993).
22. Chomczynski, P., and K. Mackey. Substitution of chloroform by bromochloropropane in the single-strip method of RNA isolation. *Anal. Biochem.* **225:**163–164 (1995).
23. Gilliland, G., K. Perrin, K. Blanchard, and H. Bunn. Analysis of cytokine mRNA and DNA: detection and quantitation by competitive polymerase chain reaction. *Proc. Natl. Acad. Sci. USA* **87:**2725–2729 (1990).
24. Gilliland, G., S. Perrin, and H. Bunn. Competitive PCR for quantitation of mRNA, in *PCR Protocols: A Guide to Methods and Applications*. Academic Press, San Diego, 60–66 (1990).
25. Xie, H., T. C. Chiles, and T. L. Rothstein. Induction of CREB activity via the surface Ig receptor of B cells. *J. Immunol.* **151:**880–889 (1993).
26. Montminy, M. R., K. A. Sevarino, J. A. Wagner, and G. Mandel. Identification of a cyclic-AMP-responsive element within the rat somatostatin gene. *Proc. Natl. Acad. Sci. USA* **83:**6682–6686 (1986).
27. Pierce, J. W., M. Lenardo, and D. Baltimore. Oligonucleotide that binds nuclear factor NF-κB acts as a lymphoid-specific and inducible enhancer element. *Proc. Natl. Acad. Sci. USA* **85:**1482–1486 (1988).
28. Lee, H. J., E. S. Masuda, N. Arai, K. Arai, and T. Yokota. Definition of *cis*-regulatory elements of the mouse interleukin-5 gene promoter. *J. Biol. Chem.* **270:**17541–17550 (1995).
29. Dunnett, C. W. A multiple comparison procedure for comparing several treatments with a control. *J. Am. Statistics Assoc.* **50:**1096–1121 (1955).
30. Schreck, R., B. Meier, D. N., Mannel, W. Droge, and P. A. Bauerle. Dithiocarbamates as potent inhibitors of NF-κB activation in intact cells. *J. Exp. Med.* **175:**1181–1194 (1992).
31. Lynn, A. B., and M. Herkenham. Localization of cannabinoid receptors and nonsaturable high-density cannabinoid binding sites in peripheral tissues of the rat: implications for receptor-mediated immune modulation by cannabinoids. *J. Pharmacol. Exp. Ther.* **268:**1612–1623 (1994).
32. Howlett, A. C. Cannabinoid inhibition of adenylate cyclase: biochemistry of the response in neuroblastoma cell membranes. *Mol. Pharmacol.* **27:**429–436 (1985).
33. Schatz, A. R., F. K. Kessler, and N. E. Kaminski. Inhibition of adenylate cyclase by Δ^9-tetrahydrocannabinol in mouse spleen cells: a potential mechanism for cannabinoid-mediated immunosuppression. *Life Sci.* **51:**25–30 (1992).
34. Shirakawa, F., M. Chedid, J. Suttles, B. A. Pollok, and S. B. Mizel. Interleukin-1 and cyclic AMP induce κ immunoglobulin light-chain expression via activation of an NF-κB-like DNA-binding protein. *Mol. Cell. Biol.* **9:**959–964 (1989).
35. Ghosh, S., and D. Baltimore. Activation *in vitro* of NF-κB by phosphorylation of its inhibitor IκB. *Nature (Lond.)* **344:**678–682 (1990).
36. Condie, R., A. Herring, W. S. Koh, M. Lee, and N. E. Kaminski. Cannabinoid inhibition of adenylate cyclase-mediated signal transduction and IL-2 expression in the murine T-cell line, EL4-IL-2. *J. Biol. Chem.* **271:**13175–13183 (1996).

Send reprint requests to: Norbert E. Kaminski, Ph.D., Department of Pharmacology and Toxicology, Michigan State University, B330, Life Sciences Building, East Lansing, MI 48824. E-mail: kamins11@pilot.msu.edu